JOM
https://doi.org/10.1007/s11837-021-04761-4

SiN_x:H Films for Efficient Bulk Passivation of Nonconventional Wafers for Silicon Heterojunction Solar Cells

ROCÍO BARRIO ,[1,2] NIEVES GONZALEZ,[1] and JOSE JAVIER GANDÍA[1]

1.—Renewable-Energy Department, CIEMAT, Avenida Complutense 40, 28040 Madrid, Spain.
2.—e-mail: rocio.barrio@ciemat.es

Hydrogenated silicon nitride films (SiN_x:H) deposited by plasma-enhanced chemical vapor deposition (PECVD) have been studied to passivate defects with hydrogen in the bulk of multicrystalline silicon wafers. Extensive analysis of the PECVD process was carried out to identify the parameters that control the SiN_x:H material composition and that mainly influence its mass density and hydrogen content. In addition, the incorporation of a hydrogen gas flow is presented as a strategy to increase the refractive index while enhancing the mass density. Satisfactory results in terms of the effective minority-carrier lifetime of the wafers have been achieved with highly hydrogenated SiN_x:H films and with slightly hydrogenated films densified by introducing a hydrogen flow, evincing the importance of the mass density in the passivation process. These hydrogenated wafers could be employed in silicon heterojunction solar cell fabrication, improving their quality, reducing their costs, and enhancing their sustainability.

INTRODUCTION

Hydrogenated silicon nitride (SiN_x:H) prepared by plasma-enhanced chemical vapor deposition (PECVD) is a highly versatile material with optical and structural properties suitable for a large number of applications.[1,2] Among these applications is the manufacture of solar cells based on the industrial diffusion technology.[3-5] The excellent optical properties of SiN_x:H allow this material to be used as an antireflective coating (ARC) in diffusion solar cells. In addition, its high hydrogen content ([H]) also enables the passivation of defects of the silicon substrate bulk, which is especially important when using multicrystalline silicon wafers (mc-Si) with a large number of defects such as grain boundaries, dislocations, and metal impurities owing to their production method.[6,7] The passivation takes place when the finished solar cells are subjected to a fast firing at temperatures above 600°C in order to form a good ohmic contact.[8] In this thermal process, some of the atomic hydrogen from the SiN_x:H diffuses into the bulk of the mc-Si wafer, passivating its defects.

(Received December 9, 2020; accepted June 8, 2021)

Published online: 28 June 2021

However, this procedure of bulk passivation cannot be used in silicon heterojunction solar cells (HIT) due to the high temperature required in the thermal treatments to passivate the defects and when firing the contacts. The reason is that the junctions of HIT cells are not formed by doping part of a solid, as is done in conventional cells based on thermal diffusion, but by deposition of thin films onto a silicon wafer at low temperature (< 250°C).[9-11]

On the other hand, the ARC layers employed in HIT solar cells must be electrically conductive to compensate for the high sheet resistance of the doped amorphous silicon emitter. For this reason, instead of dielectric SiN_x:H as ARC, high-quality transparent conductive oxides (TCO), typically degenerate semiconductors such as aluminum zinc oxide or tin-doped indium oxide, are used in HIT solar cells.[12] However, these TCOs cannot be employed for bulk passivation. In general, in this configuration with TCOs, HIT solar cells are characterized by high efficiencies of more than 26%,[13,14] mainly due to the use of excellent *n*-type monocrystalline silicon wafers, the good surface passivation, and the formation of heterostructures that allow high open-circuit voltages to be obtained.[15]

In the case of silicon heterojunction solar cells to be fabricated with mc-Si, one step of bulk conditioning must be implemented to passivate defects, but being compatible with their typical manufacturing process at low temperatures. In addition, since the junctions are formed by depositing thin layers onto the wafer surfaces in the fabrication of this type of solar cell, the cleaning and conditioning processes are of critical importance. It is thus of great interest to develop passivation methods that do not alter the surface not introduce additional cleaning steps into the manufacture process to maintain their typical high efficiency.

Taking advantage of the excellent properties of SiN_x:H, we propose herein the use of these films to passivate defects in the bulk of *p*-type mc-Si wafers as a step before the manufacture of HIT solar cells due to be necessary annealing treatments to diffuse hydrogen into silicon substrates. The SiN_x:H material was deposited by PECVD using pure silane (SiH_4) and nitrogen (N_2) instead of ammonia as precursor gases. The substitution of ammonia for nitrogen offers all the advantages implied by the use of an inert gas, greatly simplifying its implementation in PECVD equipment already installed in our laboratory.

The proposed method basically consists of depositing SiN_x:H films on both faces of the wafers. Then, the mc-Si wafers with as-deposited films are subjected to rapid thermal annealing (RTA) treatments in forming gas atmosphere to release the atomic hydrogen from the SiN_x:H layers and diffuse it through the bulk. Finally, the SiN_x:H films are completely removed by immersion in dilute hydrogen fluoride (HF:DIW) solution at room temperature, leaving the mc-Si wafer surfaces ready for deposition of the emitter and buffer layers in the later steps of the HIT solar cell manufacturing process. This method is simple and can be easily incorporated into the manufacturing stages of low-cost and more sustainable HIT solar cells. Obtaining highly efficient HIT solar cells with mc-Si wafers (after hydrogen bulk passivation) could be interesting to maintain low cost levels for photovoltaic generation installations. The procedure will be especially useful if monocrystalline silicon wafer prices rise again as they did a few years ago[16] or in case of reduced supply of monocrystalline silicon than demand. In the face of such a scenario, it may become necessary to resort to mc-Si, given the high forecasts for new photovoltaic solar energy installations over the next decade.[17]

EXPERIMENTAL PROCEDURES

Preparation and Characterization of SiN_x:H Material

To acheive efficient passivation, the SiN_x:H films must provide a sufficient amount of hydrogen, and this should be diffused throughout the bulk of the wafer during the annealing treatments. Therefore, both the optical and structural properties and the composition of the material will have an essential function in the passivation ability. Thus, an exhaustive study of the deposition process was carried out to identify which parameters critically affect the properties and composition of the material.

SiN_x:H material was deposited by a direct high-vacuum parallel-plate PECVD-MVSystem reactor at an excitation frequency of 13.56 MHz, using N_2 and pure SiH_4 as precursor gases.

For optical characterization, reflectance and transmittance spectra in the wavelength range from 300 nm to 2500 nm were obtained using an ultraviolet-visible-near infrared PerkinElmer Lambda 1050 spectrophotometer. From the spectra, the refractive index at 605 nm (n_{605}) and the film thickness were calculated for SiN_x:H deposited onto soda-lime glass substrates. The films were characterized according to procedures described in previous work.[18]

The hydrogen content [H] and its distribution in the material structure were determined by Fourier-transform infrared (FTIR) spectroscopy following standard procedures.[19-22] The infrared absorption spectra were recorded from SiN_x:H layers with thicknesses between 200 nm to 300 nm, depending on the parameters of the PECVD process, deposited on Czochralski monocrystalline silicon wafers, using a PerkinElmer Lambda Spectrum 100 FT-IR spectrophotometer. This technique provides information about the possible stoichiometry of the material based on the position and relative intensities of its characteristic bands (Si-N, Si-H, and N-H). From IR spectra, the bond densities (atm/cm^3) of the hydrogen bands were determined. The bond density relation of the hydrogen bands (defined as $R^* = \log[\text{N-H}]/\log[\text{Si-H}]$) together with the refractive index are very useful tools to estimate the stoichiometry, that is, how enriched in N atoms or Si atoms the SiN_x:H films are.

In addition, the chemical composition in bulk of some SiN_x:H films and the presence of chemical impurities were evaluated by combining x-photoelectron spectroscopy (XPS) and fixed-angle sputtering.

Hydrogenation Process and Bulk Passivation

For the passivation process, SiN_x:H layers with a thickness of 80 nm were symmetrically deposited on both sides of 1 Ω cm to 3 Ω cm *p*-type textured mc-Si wafers with thickness of 200 μm, previously laser-cut to an area of 4 cm^2. Prior to deposition, the wafers were chemically etched in 5% FH:DIW (hydrogen fluoride diluted in 18.2 MΩ cm resistivity deionized water) solution at room temperature for 5 min to remove the native oxide.

Symmetrical SiN_x:H/mc-Si/SiN_x:H structures were annealed in an RTA furnace in a forming gas atmosphere for 6 s. Distinct temperatures (650°C and 750°C) were applied to SiN_x:H films with

different compositions to establish the material properties and the annealing processes most suitable to efficiently passivate the wafer bulk. Finally, the SiN_x:H layers were completely removed with a 5% HF bath at room temperature. The bulk passivation process is shown schematically in Fig. 1.

To evaluate this hydrogen passivation process, 80-nm intrinsic amorphous silicon (a-Si:H(i)) layers were deposited on both surfaces of the as-cleaned mc-Si wafers to reduce the superficial recombination. The effective minority-carrier lifetime (τ_{eff}) and effective diffusion length (L_d) values were determined. The a-Si:H(i) films were prepared by PECVD in another vacuum chamber with the same MVS equipment employed for the deposition of the SiN_x:H material, to avoid cross-contamination. Furthermore, mc-Si wafers which were not subjected to the bulk passivation process were also introduced into the same deposition process as a-Si:H(i) for as reference. The fixed PECVD deposition parameters for the a-Si:H(i) material were pressure of P = 400 mTorr, temperature of T = 200°C, radiofrequency power (RFP) of 1 W, and silane flow of $\Phi(SiH_4)$ = 20 sccm for 15 min. These a-Si:H passivating layers have been previously optimized by using high-quality monocrystalline silicon wafers as reference, until obtaining τ_{eff} above 2.2 ms and an implicit open-circuit voltage above 750 mV.

The effective minority-carrier lifetime was extracted at the minority-carrier injection level measured by means of the quasi-steady-state photoconductance (QSSPC) technique developed by Sinton and Cuevas[23-26] using a commercial setup (Sinton Consulting WCT-120). The measurements were taken using the contactless symmetrical a-Si:H(i)/mc-Si/a-Si:H(i) structures, and the quality of the hydrogen passivation process was estimated by comparison with measurements on reference mc-Si without hydrogenation.

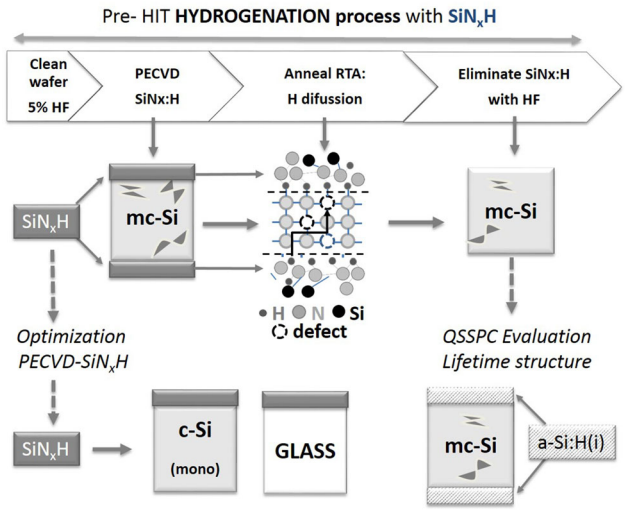

Fig. 1. Proposed passivation process with SiN_x:H before fabrication of HIT solar cells. The bottom row illustrates the steps of optimization of SiN_x:H and the evaluation of bulk passivation.

From τ, the diffusion length (L_d) was obtained using the diffusivity (D) of silicon according to Eq. 1,

$$L_d = \sqrt{D\tau} \quad (1)$$

The value of D employed was 30.44 $cm^2\ s^{-1}$ on average, as estimated from the electron mobility for p-type silicon with a doping level of 6×10^{15} cm^{-3}, obtained from the value of the resistivity of the wafers (1 Ω cm to 3 Ω cm).[27,28] L_d is a useful parameter to extract information about recombination processes in semiconductors. The goal in solar cells is to reach L_d values larger than the thickness of the absorbent (in this case, $L_d >>$ mc-Si thickness ≈ 200 μm).

RESULTS AND DISCUSSION

Study of Deposition Process of SiN_x:H Layers by PECVD

The influence of the PECVD deposition parameters on the optical and structural properties of the SiN_x:H films was analyzed. The preparation conditions on which this study focused were the ratio of the precursor gas flows ($R = \varphi(N_2)/\varphi(SiH_4)$) and the RFP. The effect of the introduction of H_2 into the mix of starting gases was also studied.

Influence of SiH_4 and N_2 Flow Ratio

One of the preparation parameters that has conventionally been considered key to control the material structure and composition is the ratio of the precursor gas flows.[29,30] Thus, two sets of samples were prepared, in which the ratio R was varied while maintaining $\varphi(SiH_4)$ fixed at 20 sccm or 5 sccm (Table I). The other deposition parameters were also kept constant (T = 260°C, P = 550 mTorr, and RFP = 80 W).

The relation of the bond densities of the hydrogen bands (R^*) and the refraction indexes (n_{605}) presented in Table I reveal that, for the deposition regimen established using these stable values of temperature, pressure, and RF power, both the material structure and optical properties were completely dominated by $\Phi(SiH_4)$. Therefore, all the samples prepared with the same $\Phi(SiH_4)$ had similar R^* and n_{605}, regardless of the $\Phi(N_2)$ used.

All films made with $\Phi(SiH_4)$ = 20 sccm were enriched in silicon, and the hydrogen atoms were preferentially linked to Si atoms, as can be deduced from the higher Si-H bond densities compared with the N-H bond densities ($R^* < 1$) and from their $n_{605} > 2$. On the contrary, when $\Phi(SiH_4)$ was as low as 5 sccm, the material obtained was N rich with $n_{605} < 2$ and N-H bond densities higher than the Si-H bond density ($R^* > 1$). Consequently, the flow relation (R) is only a key parameter to control the material composition when it is adjusted by varying $\Phi(SiH_4)$. Films deposited with similar flow relations, for example, R = 9 and R = 10, but quite distinct $\Phi(SiH_4)$ values of 20 sccm and 5 sccm, had totally

Table I. Hydrogen content [H], bond density relation R^*, and refraction indexes at 605 nm of SiN_x:H samples deposited with different flow ratios (R) at two fixed $\Phi(SiH_4)$ values

Φ (SiH_4) (sccm)	Φ (N_2) (sccm)	R	n_{605}	Si-H (at/cm^3)	N-H (at/cm^3)	R^*	[H] (%)
20	30	1.5	2.5	2×10^{22}	3×10^{21}	0.96	14
20	60	3	2.1	2×10^{22}	3×10^{21}	0.96	13
20	200	10	2.2	1×10^{22}	3×10^{21}	0.97	11
5	15	3	1.9	8×10^{20}	2×10^{22}	1.06	13
5	25	5	1.9	2×10^{21}	4×10^{22}	1.06	22
5	35	7	1.8	9×10^{20}	3×10^{22}	1.08	23
5	45	9	1.7	5×10^{20}	3×10^{22}	1.08	26
5	65	13	1.8	2×10^{21}	3×10^{22}	1.06	23

different compositions and optical properties. The explanation can be found in the difference between the stability of the SiH_4 and N_2 molecules. The Si-H bonds of SiH_4 are much weaker than the N-N triple bond of the N_2 molecule (H-Si: 393 KJ/mol; N-N: 941 KJ/mol) so that, maintaining the same applied RFP, if $\varphi(SiH_4)$ is too high, its depletion will control the deposition process and the obtained SiN_x:H will have a high proportion of Si atoms in its composition.

We also analyzed whether $\varphi(N_2)$ affected other material properties such as [H] and the mass density. In this work, the effect of the deposition parameters on the mass density was evaluated directly by comparing the Si-N main band intensities divided by the film thickness and normalized at the unit. The Si-N band intensity has been described as a reliable qualitative estimation of the mass density of a material.[31] If we focus on the samples prepared using a $\Phi(SiH_4)$ of 5 sccm, an appreciable decrease in Si-N band intensities is observed when increasing $\varphi(N_2)$ (Fig. 2), clearly indicating a reduction in mass density. [H] rose from 13% for the lowest $\varphi(N_2)$ until reaching more than 20% for the highest flows (Table I), also evidencing a less dense material.

The correlation between $\varphi(N_2)$ and the mass density is associated with the high stability of N_2 molecule. During the deposition process, N_2 molecules must remain in the space between the electrodes for long enough that the supplied power can break the strong N-N bonds and generate sufficient nitrogen radicals in the plasma. The decrease of the residence time caused by an increase of $\varphi(N_2)$ leads to the formation of fewer N radicals, which will result in a deposited material that is deficient in nitrogen atoms. Furthermore, it is possible that the SiH_4 depletion does not provide the amount of hydrogen necessary to passivate the dangling bonds of the silicon atoms not bonded to nitrogen, this being the reason why the material is not very compact. To corroborate the above, the chemical composition in the bulk of some SiN_x:H films from this series was analyzed by XPS measurements with etching in depth.

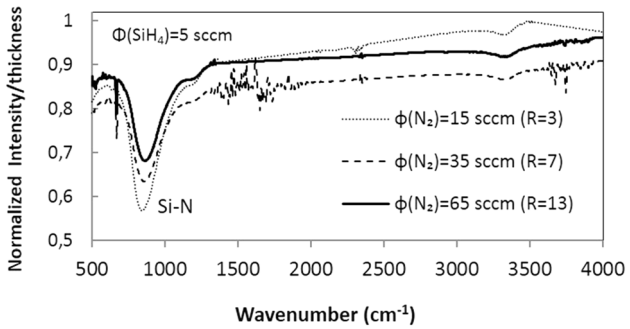

Fig. 2. Normalized FTIR spectra of SiN_x:H samples with different $\varphi(N_2)$ and fixed $\phi(SiH_4)$=5 sccm. We observe important variation of Si-N band with the $\phi(N_2)$.

Assuming that the differences between the values are small, certain trends can be seen in the percentage of the elements. When increasing $\varphi(N_2)$, the films contain a lower nitrogen percentage in their composition (N from 47 at.% to 43 at.%), which is in accordance with the decrease of the Si-N band intensity observed in Fig. 2. It is worth noting the substantial oxygen percentage in the bulk composition, possibly coming from ambient contamination,[32] which also increases as more $\varphi(N_2)$ is introduced (O from 9 at.% to 12 at.%). To verify that the film was indeed contaminated by ambient oxygen, a sample consisting of a SiN_x:H film covered by a thin a-Si:H(i) layer ($\sim$ 20 nm), deposited following the same process, was analyzed by XPS. This a-Si:H layer was intended to act as a barrier preventing oxygen penetration into SiN_x:H bulk. The SiN_x:H film covered with the a-Si:H(i) layer exhibited a significantly lower oxygen percentage (4 at.% versus 11 at.%), confirming the ambient origin of the oxygen.

In view of these results, we can say that, in the deposition regimen studied, $\varphi(N_2)$ does not practically affect the structure or optical properties of the material but has an important effect on the mass density and consequently on [H]. The deposited material is less compact and is more exposed to

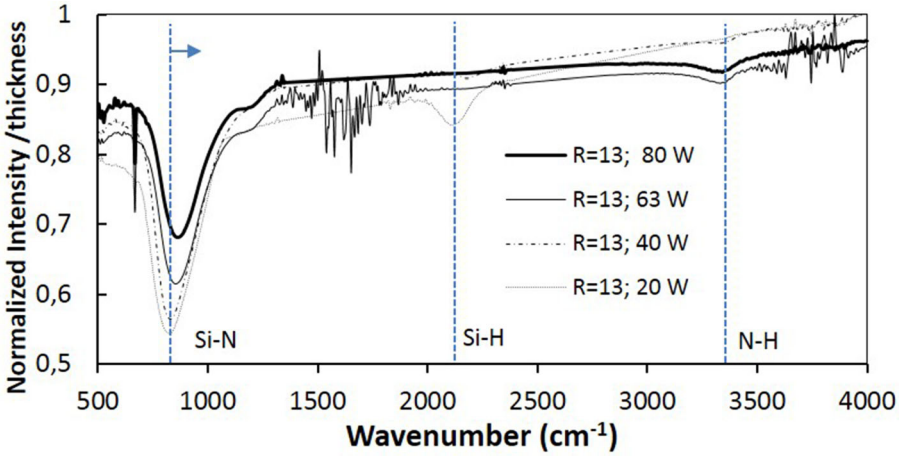

Fig. 3. FTIR spectra of SiN_x:H samples deposited by PECVD with different RF-Power, $\Phi(SH_4)$=5 sccm and $\Phi(N_2)$=65 sccm (R=13). Similar trends were observed for series with R = 7 and R = 3.

contamination by oxygen when high flows of nitrogen are introduced.

Influence of RFP

To study the effect of RFP between 20 W and 80 W (that is, 0.2 W/cm^2 to 0.8 W/cm^2), we employed a low silane flow of $\varphi(SiH_4)$ = 5 sccm to avoid the process being dominated by silane depletion, thus the deposited material could be a mixture of amorphous silicon-silicon nitride in the low power regimen.

The study was carried out at three R values (13, 7, and 3) corresponding to $\varphi(N_2)$ values of 65 sccm, 35 sccm, and 15 sccm, respectively. For all the values of R, we observed that the RFP deeply affected the material composition, as can be seen from the evolution of the bands in the FTIR spectrum (Fig. 3). Increasing RFP shifted the Si-N main band peak towards higher wavenumber due to the replacement in the lattice of Si atoms by more electronegative nitrogen atoms, which increases the Si-N bond energy. Furthermore, the hydrogen bands corresponding to the N-H bonds started to appear, while the Si-H bands vanished. These results indicate that the SiN_x:H material was enriched in nitrogen as the RFP was increased.[33]

Figure 4 shows [H] versus the ratio R^* for the three series of R assayed. The most hydrogenated films were those prepared at the lowest and highest RFP values, also corresponding to the lowest and largest values of R^*. In contrast, the films in which R^* was close to unity exhibited the lowest hydrogen contents. We observed the same trend in the three series; that is, the films with more [H] were also the most enriched in both Si (Si-rich material) and N (N-rich material).

Influence of H_2 Flow

To assess the effect of introducing H_2 into the precursor gas mixture, a set of samples was

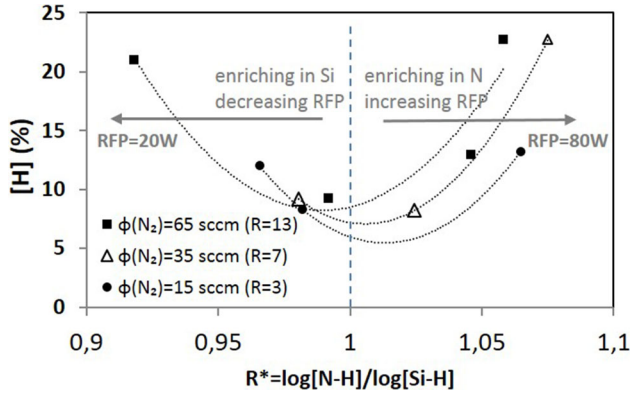

Fig. 4. Hydrogen contents versus the relation R*=log [N-H]/log [Si-H] for the three series of R with different RFP applied.

prepared with $\varphi(H_2)$ varied from 0 sccm to 35 sccm. The other deposition parameters were kept constant at R = 7 with $\varphi(SiH_4)$ = 5 sccm, RFP of 80 W, T = 260°C, and P = 550 mTorr. Incorporation of H_2 gas produced a remarkable change in both the material structure and its optical properties, achieving a material that was increasingly enriched in Si with increasing $\varphi(H_2)$. The Si-H bond intensity increased while the N-H bond intensity decreased as $\Phi(H_2)$ was increased. As a consequence, n_{605} varied from 1.8 to 2.1 and R^* decreased (from 1.08 to 0.98). For a low $\varphi(H_2)$ value of 5 sccm, significant variations in the composition were not observed, as can be seen from the similar distribution of FTIR bands and n_{605} values with respect to the sample obtained without $\Phi(H_2)$ (Fig. 5). However, the increase of the Si-N band intensity and the large reduction of [H] indicate a notable densification effect when using a $\varphi(H_2)$ value of only 5 sccm (Fig. 5, inset). The hydrogen loses its densification ability as the flow is increased, as can be deduced from the evolution of

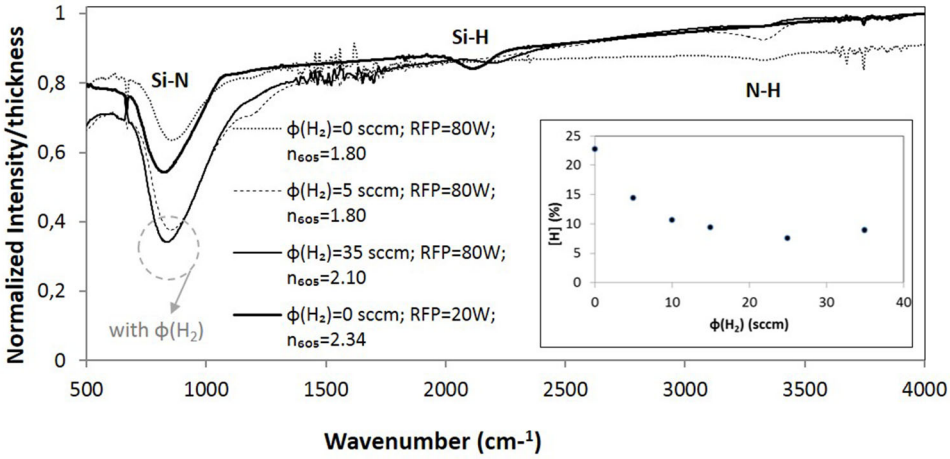

Fig. 5. Evolution of FTIR spectra and hydrogen content (inset) of SiN_x:H samples deposited by PECVD with incorporation of $\Phi(H_2)$ into the gas mixture. Incorporation of H_2 gas allowed an Si-richer material (see Si-H band) with enhanced mass density (see evolution of Si-N band) to be obtained. At a low RFP of 20 W, the Si-richer material was also obtained previously (see Si-H band).

[H] for the films with $\varphi(H_2)$, acting exclusively on their composition.

Considering these results, one can say that incorporation of H_2 gas allowed the refractive index to be adjusted to higher values, obtaining an Si-richer material with enhanced mass density. Previously, Si-rich films with $n_{605} > 2$ were also obtained by using RFP values as low as 20 W, but impairing their mass density, as seen by comparing the FTIR spectra in Fig. 5.

Bulk Passivation of Multicrystalline Silicon Wafers

As discussed above, the effectiveness of the passivation by the SiN_x:H material does not depend exclusively on its grade of hydrogenation, as the annealing processes also play an essential role. Therefore, both the annealing temperature and material properties should be chosen appropriately. For this reason, three sets of samples of SiN_x:H previously analyzed with n_{605} values of > 2.1, ~ 2, and < 1.9, where the hydrogen was preferentially bonded to Si, shared between Si and N, and preferentially bonded to N, respectively, were assayed. For each refractive index, in addition to samples with different [H], samples with distinct mass densities were also selected since this material property has been shown to greatly influence the passivation of defects, thus denser films have been reported to provide improved passivation parameters.[34-36]

In the passivation method described herein, after depositing the SiN_x:H films, the wafers were subjected to RTA processes in forming gas atmosphere. Two temperatures were studied: 650°C and 750°C. The aim is to identify which combination of RTA temperature and SiN_x:H composition provides the best passivation parameters and determine the impact of the mass density on the effectiveness of the passivation. The bulk passivation ability was estimated by QSSPC measurements once the SiN_x:H layers had been removed by immersion in diluted HF:DIW solutions at room temperature and a-Si:H(i) films had been deposited on both faces of the mc-Si wafers.

Table II summarizes the bulk passivation results for the mc-Si wafers after RTA treatment at 650°C.

For this temperature, appreciable improvements in τ and L_d were observed compared with reference values of mc-Si wafers without H passivation ($\tau_0 <$ 23 μs and $L_d <$ 173 μm). As can be seen from Table II, greater lifetimes ($\tau > \tau_0$) and diffusion lengths ($L_d >>$ thickness of mc-Si wafers $\sim$ 200 μm) values were attained with rich-Si samples with $n_{605} > 2.1$ (samples F and G). The best bulk passivation result (τ = 60 μs) was obtained when the SiN_x:H was also highly hydrogenated at [H] = 21 at.%. However, it is worth noting the lifetime of τ = 39 μs obtained with the slightly hydrogenated sample (G) with only [H] = 12 at.%. This is due to the densification caused by the incorporation of $\varphi(H_2)$ into the precursor gases (see the Si-N bands in FTIR spectra in Fig. 6). The compactness favors hydrogen diffusion in its atomic form over its molecular form, achieving more efficient passivation.[34] At 650°C, L_d above 300 μm is also achieved by using films with $n_{605} < 1.9$ and a high hydrogen content of 23 at.% (sample B).

Then, similar samples were subjected to a higher temperature (750°C) to mobilize hydrogen bonded as N-H of the SiN_x:H films with $n_{605} < 2$ and observe whether it affected the bulk passivation. After this annealing treatment, one can highlight only the result of τ = 48 μs and L_d = 381 μm, obtained using the films with high hydrogen content ([H] = 23 at.%) (sample B). However, τ was not as high as that achieved with films subjected to RTA at 650°C, even though their [H] values were comparable. This is probably due to effusion of atomic hydrogen of the

Table II. Effective minority-carrier lifetime (injection level at $N_A = 10^{-15}$ cm^{-3}) and diffusion length of H-bulk passivated mc-Si wafers after RTA treatment at 650°C for 6 s

n_{605}	Sample	R	$\Phi(H_2)$ (sccm)	RFP (W)	n_{605}	[H] (%)	τ_{eff} (μs)	L_d (μm)
< **1.9**	A	3	0	80	1.86	13	19	238
	B	13	0	80	1.80	23	32	311
	C	7	5	80	1.86	14	17	226
~ **2**	D	3	0	50	1.98	12	19	239
	E	7	15	80	1.93	9	23	263
> **2.1**	**F**	**13**	**0**	**20**	**2.34**	**21**	**60**	**424**
	G	3	16	80	2.25	12	39	342

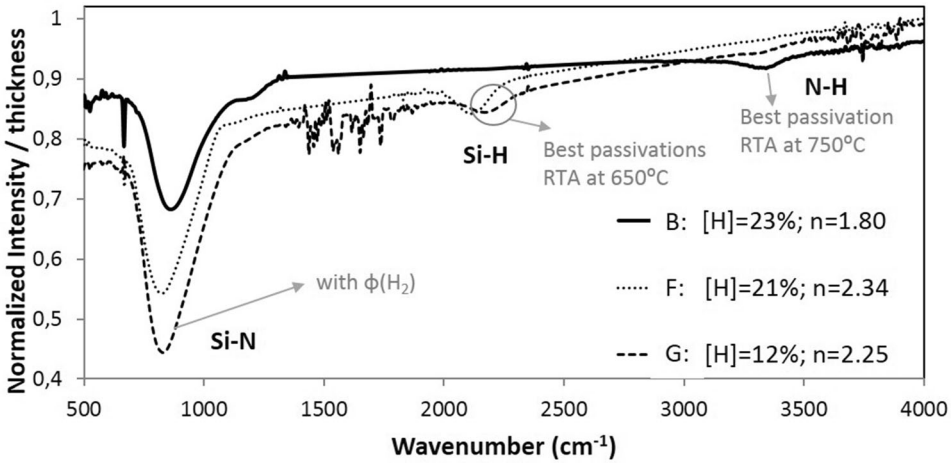

Fig. 6. FTIR spectra of SiN_x:H samples for which the best H-bulk passivation results of mc-Si wafers were obtained. Samples F and G were the best SiN_x:H for RTA at 650°C with final lifetime of 60 μs and 39 μs, respectively, for passivated mc-Si wafers. Sample B was the best SiN_x:H for RTA at 750°C with final lifetime of 48 μs for passivated mc-Si wafers.

Si-H bonds in the SiN_x:H films that are Si rich when the annealing occurs at temperatures higher than 650°C.

If we examine the best passivation results for each RTA temperature (i.e., samples B and F), we can appreciate that SiN_x:H films present a high hydrogen content. The passivation could be even better if an intense Si-N band in FTIR spectra is obtained (as for sample G with $\varphi(H_2)$), again highlighting the key role of mass density in the passivation effectiveness.

Regarding the viability of this bulk passivation method using SiN_x:H for solar cells, we achieved diffusion lengths considerably above the thickness of mc-Si wafers, so we can conclude that such mc-Si wafers, after this H-passivation process, could be used as absorbents in HIT solar cells. Furthermore, as can be inferred from these passivation values, there is not an appreciable deterioration or contamination on the surfaces of the mc-Si wafers, which is especially important for heterostructures to avoid surface recombination. Thus, no additional cleaning steps would need be introduced, and the surfaces would be ready for deposition of subsequent layers in the HIT solar cell manufacturing process.

CONCLUSION

We propose herein the use of SiN_x:H films deposited by PECVD using pure silane and nitrogen instead of ammonia as precursor gases to passivate defects in the bulk of *p*-type textured mc-Si wafers to be used as the absorber in HIT solar cells. We present a simple method consisting of deposition of SiN_x:H films on both faces of mc-Si wafers, followed by RTA treatment to release atomic hydrogen from the SiN_x:H layers and diffuse it through the bulk to passivate defects. Finally, the SiN_x:H films are completely removed, leaving surfaces ready for use in HIT solar cells.

First, based on an exhaustive study of the deposition process, we identified the N_2/SiH_4 flow ratio and the RFP as parameters having a clear impact on the structure, composition, and optical properties of the material. Regarding the flow ratio, the adjustment of the material composition is practically dominated by $\Phi(SiH_4)$. On the contrary, $\Phi(N_2)$

mainly affects the mass density and consequently [H]. The RFP strongly alters the material composition, enriching SiN_x:H with nitrogen as it increases. The films with the highest values of [H] corresponded to both Si- and N-rich materials prepared at low and high RFP values, respectively. Finally, the introduction of an additional H_2 gas flow was demonstrated to be a useful strategy to adjust the refractive index to higher values and enhance the mass density of the material.

We then estimated the bulk passivation ability of SiN_x:H films with different refractive indexes, hydrogen contents, and mass densities. The best results ($\tau \approx 60$ μs and $L_d > 400$ μm, greater than the thickness of the mc-Si wafers) were achieved by using Si-rich SiN_x:H layers that were highly hydrogenated after RTA at 650°C. For this temperature, good results were also obtained with Si-rich but slightly hydrogenated films, for which the material density was increased by introducing a hydrogen flow, evincing the importance of the mass density in the effectiveness of the passivation. Notable improvements were also observed ($\tau \approx 48$ μs) with N-rich SiN_x:H films with high hydrogen content subjected to RTA at 750°C.

Considering the results of this investigation, it can be concluded that such SiN_x:H material prepared by PECVD using N_2 gas as nitrogen source provides sufficient hydrogen and has appropriate properties to be utilized in the bulk passivation method proposed for mc-Si wafers.

Furthermore, this hydrogenation process is easily reproducible, viable, and not complicated to incorporate as a previous step in the HIT solar cell production chain based on low-cost and more sustainable mc-Si wafers.

ACKNOWLEDGEMENTS

This work has been funded by the Spanish of Ministry of Economy and Competitiveness under projects CHENOC 'Silicon HEterojunction solar cells in Non-Conventional structures' (ENE2016-78933-C4-3-R). Program Oriented to the Challenges of the Society - Spain National Plan for Scientific and Technical Research and Innovation 2013-2016. The authors would like to thank the Unit of Microstructural and Microanalysis Characterization of CIEMAT for XPS measurements and the CAI of Physic-UCM for RTA treatments.

CONFLICT OF INTEREST

The authors declare that they have no conflicts of interest.

REFERENCES

1. A.E. Kaloyeros, F.A. Jové, J. Goff, and B. Arkles, *ECS J. Solid State Sci. Technol.* 6, 691. https://doi.org/10.1149/2.0011710jss (2017).
2. C. Sun, W. Weigand, J. Shi, Z. Yu, R. Basnet, S.P. Phang, Z.C. Holman, and D. Maconald, *Appl. Phys. Lett.* 115, 252103. https://doi.org/10.1063/1.5132368 (2019).
3. F. Duerinckx, *J. Szlufcik. Sol. Energy Mater. Sol. Cells.* 72, 231. https://doi.org/10.1016/S0927-0248(01)00170-2 (2002).
4. D.H. Neuhaus, and A. Münzer, *Adv. Optoelectron.* https://doi.org/10.1155/2007/24521 (2007).
5. M. Lipiński, *Arch. Mater. Sci. Eng.* 46, 69. (2010).
6. C. Trassy, S. Martinuzzi, J. Degoulange, and I. Pe, *Sol. Energy Mater. Sol. Cells.* 92, 1269. https://doi.org/10.1016/j.solmat.2008.04.020 (2008).
7. R. Chen, H. Tong, H. Zhu, C. Ding, H. Li, D. Chen, B. Hallam, C.M. Chong, S. Wenham, and A. Ciesla, *Prog. Photovolt. Res. Appl.* https://doi.org/10.1002/pip.3243 (2020).
8. P. Panek, and M. Lipinski, *Opto-Electron. Rev.* 11(4), 269. (2003).
9. N. Jensen, R.M. Hausner, R.B. Bergmann, J.H. Werner, and U. Rau, *Prog. Photovolt. Res. Appl.* 10, 1. https://doi.org/10.1002/pip.398 (2002).
10. M. Taguchi, A. Terakawa, E. Maruyama, and M. Tanaka, *Prog. Photovolt. Res. Appl.* 13, 481. https://doi.org/10.1002/pip.646 (2005).
11. D. Chen, M. Kim, J. Shi, B. Vicari Stefani, Z. Yu, S. Liu, R. Einhaus, S. Wenham, Z. Holman, and B. Hallam, *Prog. Photovolt. Res. Appl.* https://doi.org/10.1002/pip.3230 (2019).
12. H. Park, Y.J. Lee, J. Park, Y. Kim, J. Yi, Y. Lee, S. Kim, C.K. Park, and K.J. Lim, *Trans. Electr. Electron. Mater.* 19, 165. https://doi.org/10.1007/s42341-018-0026-8 (2018).
13. K. Yoshikawa, H. Kawasaki, W. Yoshida, T. Irie, K. Konishi, K. Nakano, T. Uto, D. Adachi, M. Kanematsu, H. Uzu, and K. Yamamoto, *Nat. Energy*. https://doi.org/10.1038/nenergy.2017.32 (2017).
14. W. van Sark, L. Korte, and F. Roca, *Physics and Technology of Amorphous-Crystalline Heterostructure Silicon Solar Cells* (Springer, Berlin, 2012).
15. M. Taguchi, A. Yano, S. Tohoda, K. Matsuyama, Y. Nakamura, T. Nishiwaki, K. Fujita, and E. Maruyama, *IEEE J. Photovolt.* 4, 9. (2014).
16. A. Louwen, W. Van Sark, R. Schropp, and A. Faaij, *Sol. Energy Mater. Sol. Cells.* 147, 295. https://doi.org/10.1016/j.solmat.2015.12.026 (2016).
17. International Renewable Energy Agency - IRENA, Future of solar photovoltaic Deployment, investment, technology, grid integration and socio-economic aspects (2019). https://www.irena.org/-/media/Files/IRENA/Agency/Publication/2019/Oct/IRENA_Future_of_wind_2019.pdf.
18. R. Barrio, J.J. Gandía, J. Cárabe, N. González, I. Torres, D. Muñoz, and C. Voz, *Sol. Energy Mater. Sol. Cells.* 94, 282. https://doi.org/10.1016/j.solmat.2009.09.017 (2010).
19. N. Maley, *Phys. Rev. B* 46, 2078. (1992).
20. M.H. Brodsky, M. Cardona, and J.J. Cuomo, *Phys. Rev. B.* 16, 3556. (1977).
21. A.A. Langford, M.L. Fleet, and A.H. Mahan, *Sol. Cells.* 27, 373. https://doi.org/10.1016/0379-6787(89)90046-X (1989).
22. O. Gabriel, T. Frijnts, S. Calnan, S. Ring, S. Kirner, A. Opitz, I. Rothert, H. Rhein, M. Zelt, K. Bhatti, J.H. Zollondz, A. Heidelberg, J. Haschke, D. Amkreutz, S. Gall, F. Friedrich, B. Stannowski, B. Rech, and R. Schlatmann, *IEEE J. Photovolt.* 4, 1343. https://doi.org/10.1109/JPHOTOV.2014.2354257 (2014).
23. A. Cuevas, and D. Macdonald, *Sol. Energy* 76, 255. https://doi.org/10.1016/j.solener.2003.07.033 (2004).
24. R.A. Sinton, A. Cuevas, and M. Stuckings, *Twenty Fifth IEEE Photovolt. Spec. Conf.* 1996, 457. https://doi.org/10.1109/PVSC.1996.564042 (1996).
25. A. Cuevas, R.A. Sinton, M. Kerr, D. Macdonald, and H. Mäckel, *Sol. Energy Mater. Sol. Cells.* 71, 295. https://doi.org/10.1016/S0927-0248(01)00089-7 (2002).
26. R. Jayakrishnan, S. Gandhi, and P. Suratkar, *Mater. Sci. Semicond. Process.* 14, 223. https://doi.org/10.1016/j.mssp.2011.02.020 (2011).
27. S.M. Sze, *Physics of semiconductor devices*, 2nd edn. (Wiley, New York, 1981).
28. K.V. Shalimova, *Física de los semiconductores* (Mir, Moscú, 1975).

29. E. Herth, H. Desré, E. Algré, C. Legrand, and T. Lasri, *Microelectron. Reliab.* 52, 141. https://doi.org/10.1016/j.microrel.2011.09.004 (2012).
30. V. Verlaan, A.D. Verkerk, W.M. Arnoldbik, C.H.M. van der Werf, R. Bakker, Z.S. Houweling, I.G. Romijn, D.M. Borsa, A.W. Weeber, S.L. Luxembourg, M. Zeman, H.F.W. Dekkers, and R.E.I. Schropp, *Thin Solid Films* 517, 3499. https://doi.org/10.1016/j.tsf.2009.01.065 (2009).
31. J.F. Lelièvre, E. Fourmond, A. Kaminski, O. Palais, D. Ballutaud, and M. Lemiti, *Sol. Energy Mater. Sol. Cells.* 93, 1281. https://doi.org/10.1016/j.solmat.2009.01.023 (2009).
32. J. Hong, W.M.M. Kessels, W.J. Soppe, A.W. Weeber, W.M. Arnoldbik, and M.C.M. Van de Sanden, *J. Vac. Sci. Technol. B: Microelectron. Nanom. Struct.* 21, 2123. https://doi.org/10.1116/1.1609481 (2003).
33. J. Robertson, *Philos. Mag. B Phys.* 69, 307. https://doi.org/10.1080/01418639408240111 (1994).
34. H.F.W. Dekkers, G. Beaucarne, M. Hiller, H. Charifi, and A. Slaoui, *Appl. Phys. Lett.* 89, 211914. https://doi.org/10.1063/1.2396900 (2006).
35. H.F.W. Dekkers, L. Carnel, and G. Beaucarne, *Appl. Phys. Lett.* 89, 013508. https://doi.org/10.1063/1.2219142 (2006).
36. M. Stavola, F. Jiang, S. Kleekajai, L. Wen, C. Peng, V. Yelundur, A. Rohatgi, G. Hahn, and L. Camel, *J. Kalejs. Mater. Res. Soc. Symp. Proc.* 1210, 3–13. https://doi.org/10.1557/proc-1210-q01-01 (2010).